

# Taking advantage of hydrophobic fluorine interactions for self-assembled quantum dots as delivery platform for enzymes

Carolina Carrillo-Carrion,<sup>\*[a]</sup> Mona Atabakhshi-Kashi,<sup>[b]</sup> Mónica Carril,<sup>[a,c]</sup> Khosro Khajeh,<sup>[b]</sup> and Wolfgang J. Parak<sup>[a,d]</sup>

**Abstract:** Self-assembly of nanoparticles provides unique opportunities as nanoplatforms for controlled delivery. By exploiting the important role of non-covalent hydrophobic interactions in the engineering of stable assemblies, nanoassemblies were formed by self-assembly of fluorinated quantum dots in aqueous medium through fluorine-fluorine interactions. These nanoassemblies were able to encapsulate different enzymes (laccase and  $\alpha$ -galactosidase) obtaining encapsulation efficiencies  $\geq 74\%$ . Importantly, the encapsulated enzymes maintained their catalytic activity, following a Michaelis-Menten kinetics. Under acidic environment the nanoassemblies were slowly disassembled allowing the release of encapsulated enzymes. The effective release of the assayed enzymes demonstrated the feasibility of this nanoplatfor to be used in pH-mediated enzyme delivery. In addition, the as-synthesized nanoassemblies of ca. 50 nm diameter presented high colloidal stability and fluorescence emission, which make them a promising multifunctional nanoplatfor.

Self-assembled nanoparticles (NPs) can be used for the controlled delivery of biological molecules such as enzymes upon certain triggers, such as pH or temperature.<sup>[1-3]</sup> Non-covalent hydrophobic interactions play an important role in the organization and stabilization of many types of assembled systems.<sup>[1]</sup> However, assemblies driven by hydrophobic interactions resulting from the alkyl chains are sometimes not sufficiently stable. Non-covalent fluorine-bonding has been used in the formation of micelles based on fluorocarbon amphiphilic copolymers,<sup>[4,5]</sup> self-assembled fluorodendrimers,<sup>[6]</sup> and vesicles by using NPs coated with fluorinated ethylene glycol (EG) ligands.<sup>[7]</sup> The stability of these nanostructures was reported to be higher than expected due to the unique hydrophobicity and lipophilicity of the fluorine atoms, which confer stronger interactions than other non-covalent bonds.<sup>[8]</sup> Also, the favorable interaction between fluorine atoms and proteins has been a subject of intensive research in biomolecular recognition.<sup>[9,10]</sup> These studies pointed out a dramatic increase in the binding affinity towards most of the proteins and enzymes upon fluorine substitution.

Herein, inspired by the role of fluorine in self-assembly and its favorable interaction with proteins, we report a delivery platform for enzymes based on self-assembled fluorinated quantum dots

(QD\_F) by exploiting the strong non-covalent fluorine-fluorine and fluorine-protein interactions. First we demonstrate the self-assembly of quantum dots (QDs) in water mediated by fluorine-fluorine interactions, obtaining stable and homogeneous nanoassemblies. Second, the entrapment of enzymes inside the assemblies and their release in acidic media is studied for laccase (Lac) and  $\alpha$ -galactosidase (GLA).<sup>[11]</sup> Detailed evaluation of the enzyme performance once encapsulated and after release is also reported.

Initially, QD\_F were prepared by ligand-exchange of trioctylphosphine oxide (TOPO)-capped CdSe/ZnSQDs<sup>[12]</sup> (Fig. SI-2) with the fluorinated ligand HS-C<sub>11</sub>-(EG)<sub>4</sub>-OC(CF<sub>3</sub>)<sub>3</sub> (Fig. SI-1). After the functionalization, <sup>1</sup>H and <sup>19</sup>F NMR confirmed the presence of the ligand on the QD surface (Fig. SI-3). The selection of this ligand was based on several reasons: i) the perfluoro-tert-butyl group permits the introduction of a high amount of fluorine atoms on the outer surface of the QDs; ii) ethylene glycol units in the linker enhance the solubility, and iii) thiol group allows for binding on the QD surface, as well as on other types of NPs such as Au NPs.<sup>[13]</sup> The choice of QDs as building unit to form the nanoassemblies was based on taking benefit from their optical properties, mainly high photoluminescence intensity and very low photobleaching under intracellular conditions. However, in principle also many other NP materials could be used, for example also biocompatible materials, and in case of QDs their Cd-free counterparts are preferred.

The spontaneous self-assembly of QD\_F in aqueous solution as a result of the strong hydrophobic fluorine-fluorine interactions allowed the formation of well-defined and homogeneous nanoassemblies (QD\_F assemblies) of (46  $\pm$  5) nm in diameter as determined by transmission electron microscopy (TEM), (Fig. 1 and SI-4). High-resolution TEM showed the crystalline nature of the QDs, and together with high-angle annular dark-field scanning transmission electron microscopy (HAADF-STEM, Fig SI-4E) confirmed gaps between QDs in the assemblies. The self-assembly process was as simple as mixing the QD\_F dispersed in DMSO with water to a final ratio (v/v) of DMSO:H<sub>2</sub>O=5:95, and stirring vigorously for 1 min with a vortex mixer. It must be pointed out that attempts to form equivalent assemblies with hydrophobic TOPO-capped QDs (QD\_TOPO) or QDs coated with a similar but non-fluorinated ligand, HS-C<sub>11</sub>-(EG)<sub>6</sub>-OH (QD\_OH), were not successful, suggesting indeed that the fluorinated head -C(CF<sub>3</sub>)<sub>3</sub> in our QD\_F plays a crucial role in the nanoassembly formation through fluorine-fluorine interactions.

The hydrodynamic diameter ( $d_h$ ) of the QD\_F assemblies as determined by dynamic light scattering (DLS) was  $d_h = (44 \pm 2)$  nm. Zeta-potential values ( $\zeta$ ) were (-35  $\pm$  1) mV in water and (-10.5  $\pm$  0.4) mV in sodium acetate buffer at pH 4, to mimic acidic conditions. The reproducibility in the nanoassemblies preparation was high with a relative standard deviation  $\leq 4\%$  in terms of hydrodynamic size. Variables such as the QD\_F

[a] Dr. C. Carrillo-Carrion\*, Dr. M. Carril, Prof. Dr. W. J. Parak  
Bioengineered Particles Group, CIC biomaGUNE,  
PaseoMiramon 182, 20014 San Sebastian, Spain  
\*E-mail: carrillocarrion.carolina@gmail.com

[b] M. Atabakhshi-Kashi, Prof. Dr. K. Khajeh  
Department of Nanobiotechnology, Tarbiat Modares University  
14115-175 Tehrān, Iran

[c] Dr. M. Carril  
Ikerbasque, Basque Foundation for Science  
48011 Bilbao, Spain

[d] Prof. Dr. W. J. Parak  
Fachbereich Physik and CHyN, Universität Hamburg  
Luruper Chaussee 149, 22607 Hamburg, Germany

concentration and DMSO amount were studied by DLS (Fig. SI-5).

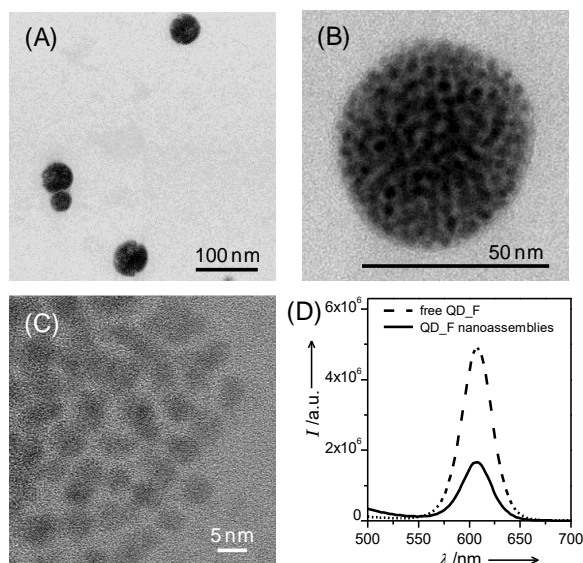


**Figure 1.** (A,B) TEM images of the nanoassemblies at different magnifications. (B) High-resolution TEM image of the assemblies showing the crystalline nature of the NPs. (D) Fluorescence emission spectra of the free QD\_F in DCM and QD\_F nanoassemblies in DMSO:H<sub>2</sub>O (5:95), both at concentration of 100 nM and recorded under excitation wavelength of 400 nm and slit widths of 2 nm.

The change in the assemblies' size with increasing QD\_F concentrations (from 25 to 250 nM) was negligible. However, the DMSO percentage had an effect on the size, obtaining larger assemblies when increasing the amount of DMSO from 5 to 20 %. As the final goal was the encapsulation of enzymes into these assemblies, we selected the minimum amount of DMSO (*i.e.* 5 %) which allowed for the formation of colloidally stable and reproducible nanoassemblies without potential unwanted effects on the enzymes. The colloidal stability of the assemblies under increasing concentrations of diverse cations and anions with biological relevance was also evaluated. Results showed no significant changes on the assemblies' size for all the studied ions up to 500 μM, and for most of them even up to 10 mM (Tables SI-2,3). For higher concentrations, the majority of the ions led to aggregation of the assemblies, except in the cases of HCO<sup>3-</sup> and HPO<sub>4</sub><sup>2-</sup> which had no effect in the whole range of concentration studied. In addition, at extreme pHs (pH 4 and 11), assemblies were only slightly larger (not aggregated) just after preparation, but the stability in time was lower, leading to larger assemblies of ca. 65 nm after 24 h (Fig. SI-6A). Further studies showed that the increase in size at pH 4 was due to the opening of the nanoassemblies, giving the chance to release the material inside. The colloidal stability of the assemblies over time stored in water at room temperature was high, observing no differences in size up to at least 30 days (Fig. SI-6B).

Subsequently, the potential of the designed QD\_F nanoassemblies as carriers for enzymes was investigated. Due to its superior robustness,<sup>[14]</sup> Lac was used as model

enzyme in the optimization of encapsulation process by monitoring the changes in the performance of the enzyme, as well as in the assemblies once Lac was encapsulated. Although Lac was here used simply as model enzyme, it must be pointed out the high relevance of laccases in a multitude of biotechnological processes<sup>[14]</sup> and their immobilization is under continuous investigation for improving their performance.<sup>[15]</sup> The encapsulation process of the enzyme within the assemblies involved two steps: i) the incubation of enzyme with QD\_F in DMSO/H<sub>2</sub>O. It is hypothesized that the enzyme molecules are adsorbed on the QD\_F surface through hydrophobic interactions between the fluorine atoms and the hydrophobic domains of the enzyme. ii) The formation of assemblies by addition of water to decrease the amount of DMSO in the mixture down to 5 %, followed by vigorous stirring for 1 min. During this step the enzyme molecules previously adsorbed on the QD\_F are entrapped within the assemblies, leading to the formation of nanoassemblies containing the enzyme encapsulated (Enz@QD\_F, Fig. 2). Using Lac enzyme, variables such as the initial ratio between NPs and Lac, incubation time, temperature, and purification protocol were optimized in order to achieve the highest encapsulation efficiency, while maintaining the maximum catalytic activity of the enzyme once encapsulated. Results of enzymatic activity and protein quantification assays clearly indicated the presence of Lac in the assemblies and allowed its quantification (SI for details).

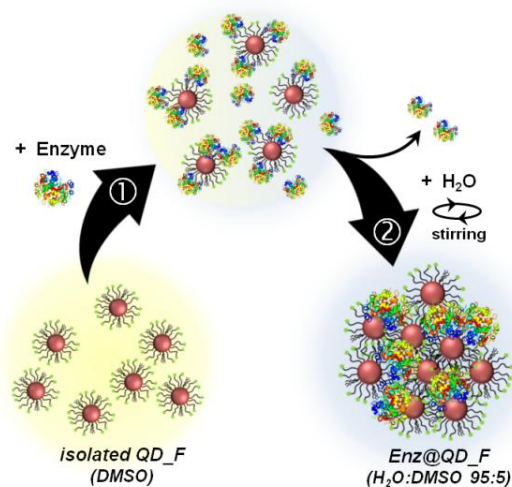


**Figure 2.** Schematic representation of the enzyme encapsulation process.

In order to compare different strategies of immobilization, Lac was covalently attached to QD\_F before assembly formation. Hence, the presence of a reactive group on the surface of the QD\_F was required and therefore QDs were prepared containing both, the fluorinated ligand (for assembly) and a carboxylated ligand (for covalent binding) (QD\_F/COOH). The activity of the covalently attached enzyme was 0.0098 U/mg (see SI), which is about 17 times lower than the specific activity S obtained for the encapsulated Lac. This result is in agreement with numerous reports showing that covalent immobilization affects strongly the activity of enzymes, either because denaturation or binding to the active site of the

enzyme.<sup>[16]</sup> Thus, immobilization based on physical entrapment of the enzyme within the assemblies was the approach used in this work.

To go a step further in the possibility of using these nanoassemblies as delivery systems, GLA was selected. GLA is an enzyme which is used in the treatment of Fabry disease.<sup>[11]</sup> GLA was encapsulated following a similar approach to that employed with Lac, although it must be noted that the encapsulation process needs to be optimized for each particular enzyme as different enzymes differ in size, conformation and sensitivity to aggregation and denaturation (SI for details).

Nanoassemblies with and without encapsulated enzymes were subjected to a comprehensive characterization. QD\_F assemblies presented high fluorescence (wavelength of excitation/emission  $\lambda_{exc}/\lambda_{em}=400/605$  nm), although lower than that of the isolated QD\_F dispersed in DCM (Fig. 1D). This was expected considering the change of medium from organic solvent to mainly aqueous medium. However, the fact that there was no drastic decrease in fluorescence when the QD\_F were assembled indicates that they are not in too close contact due to the fluorinated ligand on their surface, and therefore, quenching effects are negligible. Interestingly a photoactivation process was observed under continuous irradiation of the assemblies with the excitation source (Fig. SI-4F). Such photoactivation is an already reported effect of the smoothing of the QD surface due to passivation of surface defects.<sup>[17]</sup>

Properties related to the nanoassemblies (*i.e.* size, and charge) and those related to the enzymes (*i.e.* encapsulated amount, specific activity, and kinetic parameters) were determined for both Lac and GLA and are summarized in Table 1.

**Table 1.** Characterization parameters of nanoassemblies without (QD\_F) and with Lac or GLA (Lac@QD\_F or GLA@QD\_F), as well as those for the free enzyme (Lac and GLA) in acetate buffer 10 mM pH = 4. Data are expressed as mean value  $\pm$  SD (n=3).

	QD_F	Lac@QD_F	Lac	GLA@QD_F	GLA
$d_h$ [nm]	47 $\pm$ 2	46 $\pm$ 2	—	53 $\pm$ 3	—
$\zeta$ [mV]	-10.5 $\pm$ 0.4	-9.0 $\pm$ 0.3	—	-9.8 $\pm$ 0.7	—
$m_{enz/sample}$ [ $\mu$ g]	—	148 $\pm$ 15	—	16.5 $\pm$ 2.2	—
S [U $\cdot$ mg <sup>-1</sup> ]	—	0.17 $\pm$ 0.01	0.26 $\pm$ 0.01	2.10 $\pm$ 0.07	5.55 $\pm$ 0.08
$K_M$ [mM]	—	1.18 $\pm$ 0.09	0.38 $\pm$ 0.03	5.8 $\pm$ 0.2	1.48 $\pm$ 0.08
$v_{max}$ [ $\mu$ mol $\cdot$ min <sup>-1</sup> $\cdot$ mg <sup>-1</sup> ]	—	0.189 $\pm$ 0.004	0.288 $\pm$ 0.006	3.2 $\pm$ 0.1	5.46 $\pm$ 0.09
$k_{cat}$ [s <sup>-1</sup> ]	—	0.208	0.317	131	229
$k_{cat}/K_M$ [s <sup>-1</sup> $\cdot$ mM <sup>-1</sup> ]	—	0.176	0.834	22	155

There were no significant changes in size and charge of the assemblies after the encapsulation of enzymes, which serves also as an indication that the enzymes are encapsulated inside the assembly and not adsorbed on their surface. Enzyme loading per assembly sample, which contains  $1\cdot 10^{-10}$  moles of QD\_F, was determined to be  $m_{enz/sample} = (148 \pm 15)$   $\mu$ g for Lac and  $(16.5 \pm 2.2)$   $\mu$ g for GLA. These amounts correspond to encapsulation efficiencies (EE) as high as 74 % and 82 % for Lac and GLA, respectively, defined as the percentage of encapsulated enzyme with respect to the total amount of

enzyme added (SI for details). The specific activity within the assemblies was calculated to be  $(0.17 \pm 0.01)$  U/mg for Lac and  $(2.10 \pm 0.07)$  U/mg for GLA (see SI). Like the free enzymes, also the encapsulated enzymes followed the kinetics of the Michaelis-Menten model (Fig. SI-7), but there were significant changes of the values of the kinetic parameters such as the Michaelis-Menten constant ( $K_M$ ), the maximal velocity ( $v_{max}$ ), the turnover rate ( $k_{cat}$ ), and the catalytic efficiency ( $k_{cat}/K_M$ ).

This is not surprising, given that the kinetic behavior of encapsulated enzymes is normally altered owing to the modification of their microenvironment, observing generally higher  $K_M$  and lower  $V_{max}$  values than those of the free enzyme.<sup>[18]</sup> In our case both encapsulated enzymes presented an apparent  $K_M$  value higher than the free forms, indicating an apparent lower affinity for the substrate. This might be attributed to limited accessibility of substrate molecules to the active sites of the enzyme and/or structural changes of the encapsulated enzyme.<sup>[19]</sup> Large increases in  $K_M$  have been also associated to a high-density-encapsulated environment,<sup>[20]</sup> and this might also be the case owing to the high amount of enzyme encapsulated within the assemblies. On the contrary,  $V_{max}$  decreased for the encapsulated enzymes, probably due to diffusional constraints.<sup>[21]</sup> The catalytic efficiency based on  $k_{cat}/K_M$  value was significantly lower for the encapsulated forms, as expected, again presumably due to a combination of the factor mentioned above. In spite of these changes observed in the encapsulated enzymes, one must keep in mind that these encapsulated enzymes will finally act once released. Subsequently, release studies of the encapsulated enzymes from the assembly were performed at pH = 4. Fig. 3 shows the effective release of Lac or GLA from the assemblies, showing that about 50% of them was released within 24 h (see SI for calculation of the release parameter R).

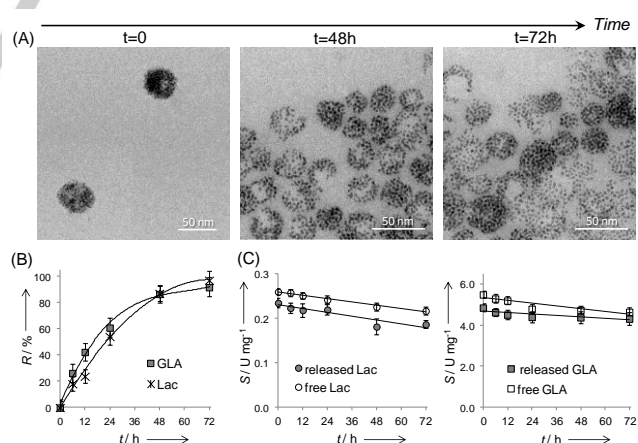


**Figure 3.** (A) TEM images over time of Lac@QD\_F dispersed in acetate buffer 20 mM at pH 4. (B) Profiles of the enzyme release (R) for Lac and GLA in acetate buffer solution 20 mM at pH 4. (C) Specific activity S of enzymes after release, as well as the evolution of the activity of free enzymes in the same medium. Data are plotted as mean value  $\pm$  SD (n=3).

It is interesting to note that when the nanoassemblies were dispersed in buffer solution at pH = 7, the release of enzymes was negligible within 48 h. TEM images of the assemblies as

they disassemble were taken at different time points. As shown in Fig. 3A the nanoassemblies are disrupted at pH = 4 and partially opened over time, allowing the release of Lac or GLA. Importantly, both enzymes retained their activity after release. As control, the stability of the free enzymes under the same conditions was also tested, showing no significant decrease in activity (Fig. 3C). From these results it can be concluded that both enzymes have a good stability within the assemblies, maintaining their activity once released.

To sum up, the herein presented QD\_F nanoassemblies display an interesting combination of advantages, namely simple, fast and very reproducible preparation, high colloidal stability, effective enzyme loading and release, and fluorescence imaging potential. The main achievements of this work could be summarized as follows: (i) Proof of the potential of non-covalent fluorine-fluorine interactions as driving force for the self-assembly of NPs, and (ii) Demonstration of the ability of this system to carry and deliver enzymes in a controlled fashion.

In this realm, we envisage the increasing use of fluorine-based non-covalent interactions for simple and reproducible self-assembly of nanoparticles as a straightforward strategy for encapsulation and release of biomolecules and drugs, in particular those sensitive to degradation or hydrophobic. Further experiments following the fate of such nanoassemblies inside cells taking advantage of QD fluorescence and potential therapies based on enzymes are of interest for the continuation of this work.

## Acknowledgements

This work was funded by MINECO (CTQ2015-68413-R to MC and MAT2013-48169-R to WJP) and the German Research Society (DFG, grant PA 794/25-1). CCC acknowledges MINECO for a Juan de la Cierva-Incorporación contract. MA acknowledges Tarbiat Modares University and Biotechnology Development Council of Iran (grant No: 950709). MC acknowledges Ikerbasque for a Research Fellow Position. We thank Marta Gallego for assisting with the TEM imaging and Jorge Blanco for contributing to the ligand synthesis.

**Keywords:** fluorine interaction • self-assembly • quantum dots • nanoassemblies • enzyme delivery

- [1] W. Cui, J. Li, G. Decher, *Adv. Mater.* **2016**, *28*, 1302-1311.
- [2] A. Yahia-Ammar, D. Sierra, F. Mérola, N. Hildebrandt, X. Le Guével, *ACS Nano* **2016**, *10*, 2591-2599.
- [3] A. A. Homaei, R. Sariri, F. Vianello, R. Stevanato, *J. Chem. Biol.* **2013**, *6*, 185-205.
- [4] H. Hussain, K. Busse, J. Kressler, *Macromol. Chem. Phys.* **2003**, *204*, 936-946.
- [5] S. D. Xiong, L. Li, J. Jiang, L. P. Tong, S. Wu, Z. S. Xu, P. K. Chu, *Biomaterials* **2010**, *31*, 2673-2685.
- [6] H. Wang, Y. Wang, Y. Wang, J. Hu, T. Li, H. Liu, Q. Zhang, Y. Cheng, *Angew. Chem.* **2010**, *54*, 11647-11651.
- [7] K. Niikura, N. Iyo, T. Higuchi, T. Nishio, H. Jinnai, N. Fujitani, K. Ijro, *J. Am. Chem. Soc.* **2012**, *134*, 7632-7635.

- [8] V. Percec, M. Glodde, G. Johansson, V. S. K. Balagurusamy, P. A. Heiney, *Angew. Chem.* **2003**, *42*, 4338-4342. [9] P. Zhou, J. Zou, F. Tian, Z. Shang, *J. Chem. Inf. Mode* **2009**, *49*, 2344-2355.
- [10] J. Pollock, D. Borkin, G. Lund, T. Purohit, E. Dyguda-Kazimierowicz, J. Grembecka, T. Cierpicki, *J. Med. Chem.* **2015**, *58*, 7465-7474.
- [11] J. Hsu, D. Serrano, T. Bhowmick, K. Kumar, Y. Shen, Y. C. Kuo, C. Garnacho C, S. Muro, *J. Control. Release* **2011**, *149*, 323-331.
- [12] J. Hühn, C. Carrillo-Carrion, M. G. Soliman, C. Pfeiffer, D. Valdeperez, A. Masood, I. Chakraborty, L. Zhu, M. Gallego, Y. Zhao, M. Carril, N. Feliu, A. Escudero, A. M. Alkilany, B. Pelaz, P. d. Pino, W. J. Parak, *Chem. Mater.* **2017**, *29*, 399-461.
- [13] O. Michelena, D. Padro, C. Carrillo-Carrion, P. Del Pino, J. Blanco, B. Arnaiz, W. J. Parak, M. Carril, *Chem. Comm.* **2017**, *53*, 2447-2450.
- [14] D. M. Mate, M. Alcalde, *Microbiotechnol.* **2016**, *10.1111/1751-7915.12422*
- [15] M. Asgher, M. Shahid, S. Kamal, H. M. N. Iqbal, *J. Mol. Catal. B: Enzym.* **2014**, *101*, 56-66.
- [16] A. A. Homaei, R. Sariri, F. Vianello, R. Stevanato, *J. Chem. Biol.* **2013**, *6*, 185-205.
- [17] C. Carrillo-Carrion, S. Cárdenas, B. M. Simonet, M. Valcárcel, *Chem. Commun.* **2009**, *35*, 5214-5226.
- [18] B. Krajewska, Z. Piwowarska, *Biocatal. Biotransform.* **2005**, *23*, 225-232.
- [19] Y. I. Doğaç, M. Çinar, M. Teke, *Prep Biochem Biotechnol.* **2015**, *45*, 144-57.
- [20] J. D. Fiedler, S. D. Brown, J. L. Lau, M. G. Finn, *Angew. Chem.* **2010**, *49*, 9648-9651.
- [21] S. A. Rothwell, S. J. Killoran, R. D. O'Neill, *Sensors* **2010**, *10*, 6439-6462.

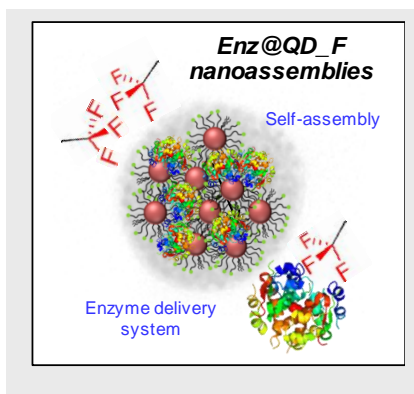
Entry for the Table of Contents (Please choose one layout)

Layout 1:

## COMMUNICATION

Text for Table of Contents

Self-assembly of quantum dots driven by fluorine-fluorine interactions are able to efficiently carry and deliver enzymes in a controlled fashion, *i.e.* pH-mediated enzyme delivery.



Author(s), Corresponding Author(s)\*

Page No. – Page No.

Title